Anomalous Etching Kinetics of Self-Assembled Monolayers on Silica−Water Interfaces: Experiment and Modeling

Xiaolin Zhao, Andrew Yen, and Raoul Kopelman*

Department of Chemistry, University of Michigan, Ann Arbor, Michigan 48109

Received: August 12, 1997[⊗]

We have studied the etching of siloxane/silica self-assembled monolayers in basic alcohol solutions using second harmonic generation. The kinetics of the etching process takes an unusual algebraic power law time dependence, with an exponent of 0.5. On the basis of the chemical nature of our system, we propose a surface cleavage mechanism and a *surface* diffusion based reaction model. We also perform Monte Carlo simulations on the system. When the solvent shell effect is considered as a geometric constraint for surface adsorption, we reproduce the anomalous power law.

Chemistry at a silica surface or interface is an important field, related not only to some traditional applications, such as chromatography and electrophoresis, but also to surface adhesion and to microelectronic structures in silicon wafers.[1−8] This work concerns *surface* diffusion, which plays an important role in many aspects of heterogeneous catalysis, in addition to semiconductor film growth and etching. Our surface kinetics measurements are based on the in situ surface second harmonic generation (SHG). SHG, as a surface-specific spectroscopic technique, is capable of measuring the surface charge density at the silica/silicon interface.[9] Based on our experimental measurements on a silica/alcohol interface reaction, a new physical picture for the surface diffusion limited reaction is proposed, which is further supported by our Monte Carlo diffusion limited surface reaction simulations. We specifically focus on the mechanism of removal of the silyl bonds linking the surface and self-assembled monolayer molecules. The system encountered is not a purely two-dimensional system, and the material at the surface is not confined to the surface: it is deposited or adsorbed from the bulk, and it can also desorb back into the bulk. This greatly complicates the reaction kinetics.

The sample prism was cleaned through lengthy soaking in clean basic and acid solutions and then baked at ∼300 °C for more than 3 h. $(CH_3)_3Si-N(CH_3)_2$ was then injected into the oven with the sample prism. We chose to use $(CH_3)_3Si-N(CH_3)_2$ as SAM because it contains only a single functional group, which eliminates the possibility of cross-linking. The sample was allowed to react for $^1/_2$ h. The prism, after cooling in vacuum, was glued to form a sample cell with one side as the sample. The contact angle of such a prepared SAM sample is 90°, indicating the existence of the silane self-assembled monolayer though not complete coverage. Previous studies show that the SAM surface coverage is about 50% of total surface sites (see Appendix).[9] The basic alcohol solution is known[10] to remove the surface Si−O−Si bonding, i.e., the self-assembled monolayer, and, therefore, increase the number of surface silanol functional groups, i.e., the surface negative charges, when exposed to a basic solution. The increase of surface charge density is monitored by optical second harmonic generation (SHG). At time zero 0.5 M KOH/MeOH solution was injected into the cell. The 532 nm light output from a 10 Hz Quanta-Ray Nd:YAG laser, with 10 ns pulse width, is used as the fundamental excitation light source. The light beam is focused into the prism through one of its side faces in a total internal reflection geometry using a 1 m focal length lens. The reflected beam exits the other side face and passes through filters (a $CoCl_2$ solution and a Melles Griot UG5 filter) and a monochromator, and the second harmonic intensity at 266 nm is measured by a Hamamatsu photomultiplier tube (PMT). The signal is averaged for 200 laser pulses, using a digital oscilloscope. The oscilloscope's internal 1 MΩ impedance results in a sufficient signal voltage and an extended decay time so that many decay points can be digitized per laser pulse. The uncertainty of the measurement is less than 5% of the SHG intensity and is mainly due to laser power fluctuations.

The SHG signal from a silica surface has been studied before in great detail and demonstrated to be a good probe for the silica surface charge density.[11,12] In general, for a charged surface, the SHG field $E(2\omega)$ takes the following form with the electric potential Ψ at the charge plane:

$$E(2\omega) = A + B\Psi([\mathrm{SiO}-]) \tag{1}$$

where A is proportional to the second-order susceptibility $\chi^{(2)}$ of the surface and B is proportional to the third-order susceptibility $\chi^{(3)}$ of the solvent.

Assuming that a constant capacitor model[13] for the interface electric potential is justified at very high ionic strength, one gets the proportionality $\Psi([\mathrm{SiO}-]) \sim [\mathrm{SiO}-]$. Also, breaking up the A ($\chi^{(2)}$ contribution) term into a contribution from the [SiO−] and a contribution from [SAM], and considering that the total number of surface sites is conserved, i.e., [SAM] + [SiO−] = N_{total}, while defining $N(t)$ as the concentration of [SiO−] at time t, one gets from eq 1

$$\begin{aligned} E(2\omega,t) &= A_1[\mathrm{SiO}-] + A_2[\mathrm{SAM}] + B\Psi([\mathrm{SiO}-]) \\ &= A_1N(t) + A_2(N_{\mathrm{total}} - N(t)) + B'N(t) \\ &= (B' + A_1 - A_2)N(t) + A_2N_{\mathrm{total}} \end{aligned} \tag{2}$$

where B', A_1, and A_2 are constants. Knowing that [SiO−] = $N(0)$ at time 0, [SiO−] = $N(t)$ at any intermediate time, and [SiO−] = $N(\infty) = N_{\mathrm{total}}$ at time ∞, one easily gets the following

* To whom correspondence should be addressed.

[⊗] Abstract published in *Advance ACS Abstracts,* November 1, 1997.

S1089-5647(97)02633-3 CCC: $14.00

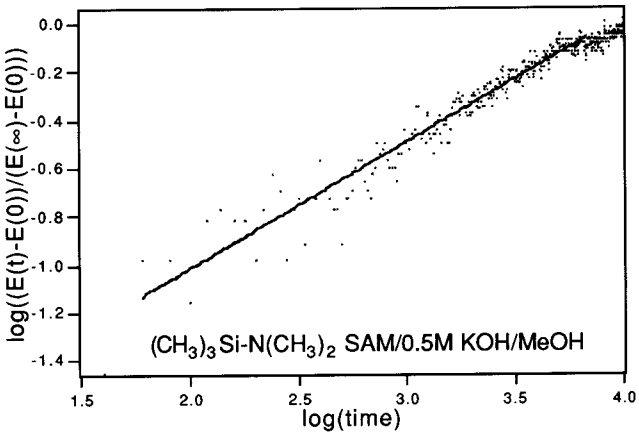

Figure 1. Second harmonic generation signal increment as a function of time (unit: seconds) after basic alcohol solution is injected. The log−log plot shows a power law dependence with a slope of 0.5. The points are the experimental results, and the line is the best linear (R = 0.97) fit to the log−log plot.

relationship

$$\frac{E(t) - E(0)}{E(\infty) - E(0)} = \frac{N(t) - N(0)}{N(\infty) - N(0)} = \frac{N(t) - N(0)}{N_{\text{total}}(1 - N(0)/N_{\text{total}})} \quad (3)$$

The term in the numerator is the net charge created during the etching process while the term in the denominator is the total SAM population at the surface. Note that $N(0)/N_{\text{total}}$ can be evaluated from the pH response curve at very high pH.

The kinetics result for the etching process is shown in Figure 1. It shows a $t^{1/2}$ power law dependence. Specifically, we observe a 0.48−0.54 slope for log($(E(t) - E(0)/E(\infty) - E(0)$) vs log(time). For most runs, this power law extends at least 2 decades in time. As we have shown, this SHG signal increase (as a function of time) is related to the total fraction of SAM removed (as a function of time). We thus need a reasonable model to explain this result.

It is difficult to explain the above result using a classical 2-D surface reaction model as the later cannot give a power law of 0.5. We thus tried to understand this phenomenon in the context of a reaction−diffusion model. Based on a model by Frish and Mysels,[14] $N \sim \rho(Dt/\pi)^{1/2}$ is the total charge created by ion diffusion from the bulk, where ρ is the density of the solute (OH^- in our case) in the bulk solution and D is the diffusion coefficient. Using the Frish model, we estimate the diffusion constant to be on the order of $D \sim 10^{-15}$ cm^2/s, a number 9−10 orders of magnitude smaller than the 10^{-6}−10^{-5} cm^2/s diffusion constant expected for OH^- in MeOH. While the electric field on the surface is expected to slow the diffusion from the bulk to the surface and thus would give a smaller "effective" diffusion coefficient, our calculation shows that the Frish power law is broken when the electric field effect is introduced and thus does not give a $t^{1/2}$ time dependence.

From previous studies[9] the coverage of the SAM is roughly 50% (see Appendix). This is consistent with the chemical nature of the SAM ending group ($-Si(CH_3)_3$). The steric effect[15] of the $-Si(CH_3)_3$ provides shielding for the underneath Si−O−Si bond and therefore makes the direct attack of OH^- from bulk unfavorable. The large volume of the ending groups also makes full surface coverage impossible. The molecular modeling indicates that the maximum surface coverage is somewhere between 30% and 50%. Therefore, there are plenty of empty sites to allow OH^- ions to adsorb directly onto the surface. On the basis of the chemical nature of our system, we propose a 2-D reaction−diffusion model, assuming the surface to be locally flat. Under this model, the OH^- first adsorbs onto the surface. This is a fast step. The adsorbed OH^- then diffuses on the 2-D surface and reacts with the siloxane monolayer, breaking up Si−O−Si bonds. From a chemical reaction point of view this is acceptable, because reaction of the SAM's ending group ($-Si(CH_3)_3$) with OH^- is unlikely. The OH^- is more likely to break up the Si−O−Si bonds. The gas-phase SAM formation at the silica surface can be regarded as resulting in a random deposition of silane (A) onto the surface. During the etching, OH^- (called B) cleaves the Si−O−Si bonding, resulting in the silane (A) leaving the surface. This is equivalent to an A + B → 0 reaction in 2-D, with a finite number of A's that are consumed throughout the reaction and with a number of B's (OH^-) that are proportional to the number of surface empty sites. While B is consumed in the reaction, the surface adsorption from the bulk compensates for the B's lost in the reaction.

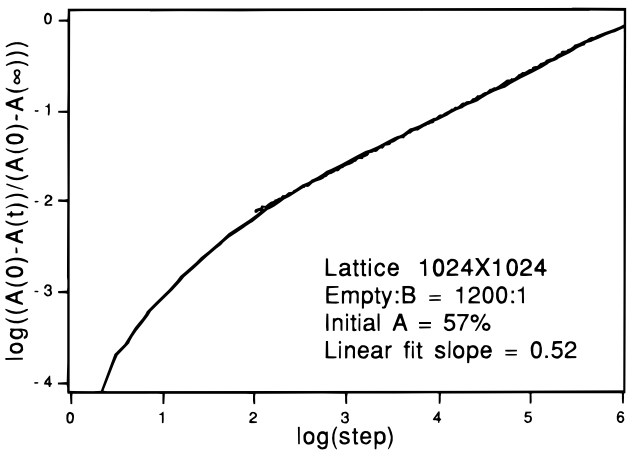

Figure 2. Simulated SAM loss vs time using 2-D diffusion−reaction model (described in the text). The log−log plot also shows a power law dependence with a slope of 0.52 (R = 0.999), and the square landing constraint is imposed with an initial surface coverage of 57%.

We have to consider the surface adsorption mechanism. First of all, the surface concentration of B cannot be too high, because OH^- is negatively charged, and therefore, in the case of our sample, the repulsive interaction with the negatively charged surface will most likely kick it away. Therefore, we assume that the surface population of B is small.

In Langmuir type surface adsorption,[13] the number of particles landing on the surface is proportional to the number of empty sites at the surface (and the number of particles leaving the surface is proportional to the number of occupied sites). It is this condition that forced us to impose a fixed ratio between the total number of the surface empty sites to the number of B particles; i.e., the adsorption is still in the linear, unsaturated range of the Langmuir type adsorption. As the A(monolayer) is consumed, more surface empty sites become available, and then the number of B's at the surface has to be adjusted to fulfill the adsorption condition, i.e., keeping the ratio between the number of B particles and number of empty sites the same.

The free energy of the adsorption is related to the species solvation energy in the bulk and at the surface. In solution adsorption, when a molecule lands on the surface from the bulk, it has to break up the solvent shell and become solvated at the surface. The energy difference of the above process makes up the free energy in the Langmuir adsorption. Suppose that there are two different domains at the surface, labeled D1 and D2; then the adsorption on these two patches will be different, because the surface solvation could be very different. In our simulation, we imposed a solvent shell for each B landing onto the surface. When B is on the surface, the case of a B landing

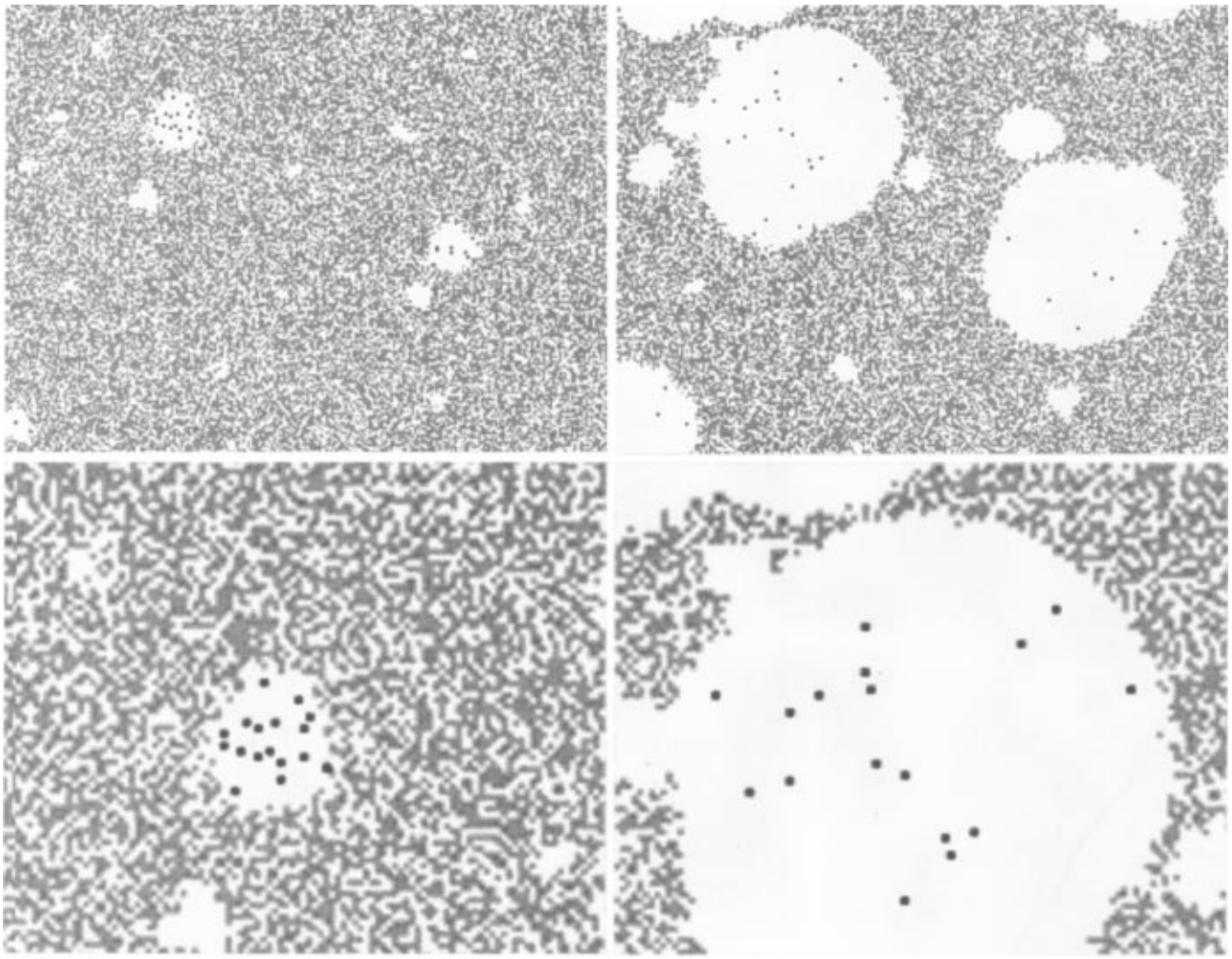

Figure 3. Surface patterns (partial) generated from the Monte Carlo simulation at two different time steps. The *left* is at step = 1000 and the *right* is at step = 10 000. The black color stands for the B random walker and the gray color stands for fixed A, while the white color stands for the empty sites. The bottom figures are magnifications of the upper left portions of the top figures.

with no A in the neighborhood (so that B lands in an empty domain) will be quite different from the case where B has an A as a nearest neighbor (so that B lands in a region where mostly there are A patches). This translates into the solvation energy difference. Therefore, we can bias the landing of B by geometrical constraints. Wherever B lands onto a surface, we draw a square around B and make sure that the landing of B should exclude the A in these nearest square. We called it a *square forbidden landing* of B, also called hard square model.[16] The model described above, although simple, should carry the essential physics of the adsorption process with its solvation difference.

The simulation starts with a fixed amount of A, randomly landed onto a 1024 × 1024 lattice. We tried initial A coverages of half of the total lattice sites. The A particle never moves; only B is doing the random walking. If B encounters an A in a move, both are removed. After all the B particles are moved once in a step, the ratio between the number of B particles and number of empty sites is examined again, and lost B is compensated for by landing more B particles so as to maintain this ratio.

We monitored the total number of A (SAM) removed as a function of time steps (to compare with our experimental data). We perform Monte Carlo simulation[17−19] with a variety of initial A (SAM) coverage. When we impose a *square forbidden landing* of B, with initial A population as 57% of the total sites, the $\log(A(0) - A(t)/A(0) - A(\infty))$ vs log(time steps) shows a power law of 0.52 that extends over 4 decades in time. The data are averaged over five runs.

It is interesting to see the surface configuration during the simulation.[20] In Figure 3, we show the etching pattern at two different time steps during the simulation. From the patterns at different times we conclude that as time progresses the different size pores grow larger and merge—a mechanism that can be described as "hole growth and fusion". The surface configuration at step = 1000 (∼1% A removed) already shows some degrees of "hole fusion", while the configuration at step = 10 000 (∼10% A removed) simply indicates a pore growth and merger. Clearly, one should not have the mean field result expected from random mixing. Currently, we are investigating the origin of the power law time dependence and its relation to the surface configuration during etching. We should note here, though, that our simulations show that the time power of 0.5 results from an interplay between the initial A deposition and the B shell landing. The initial A concentration does not have to be 50% to show the power of 0.5 time dependence. A more detailed paper account on the simulations will appear in a separate publication.

In summary, we explain the unusual power law of the etching process with a surface diffusion limited reaction model. We show that when a geometric constraint is imposed on the landing process, and with an initial coverage of SAM close to 50%,

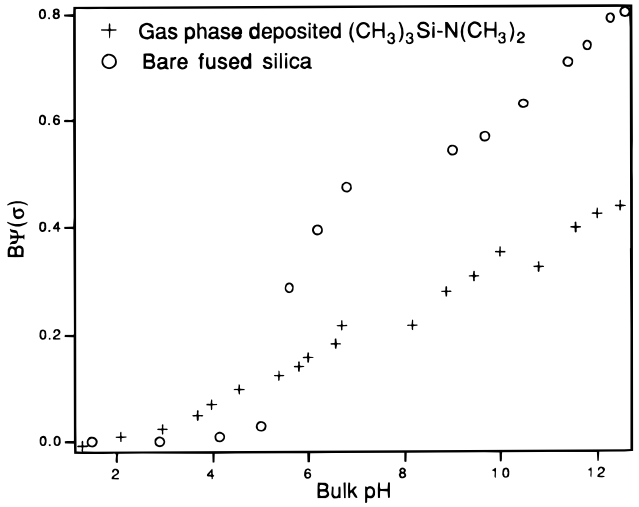

Figure 4. pH-dependent part of the second harmonic generation signal for bare silica and for a $(CH_3)_3-Si-N(CH_3)_2$ self-assembled monolayer (SAM)-covered silica sample. Note that at high pH (∼13) the signal value for the SAM-covered sample is roughly half that of the bare silica.

which is consistent with the chemical nature of our system, the Monte Carlo simulations show a behavior similar to that obtained experimentally. The excellent agreement between our experiment and the simulation indicates that we have a self-consistent model for the cleavage mechanism and kinetics.

Acknowledgment. We thank Prof. C. Evans for the use of the contact angle apparatus. We acknowledge support from the National Science Foundation, Grant DMR 9410709.

Appendix

The surface coverage of SAM can be determined from the $B\Psi([\sigma])$ vs pH dependence curve.[11] The compound chosen for the present study is the mono-*N*,*N*-dimethylamino *leaving group*, because the monofunctional nature of the organosilane permits only a single bond between the silane and the surface. Cross-linking and polymerization are impossible for the monofunctional silanes. It should be noted that the silane, once linked to the surface, should effectively terminate the original silanol functional group, making it inert to bulk pH changes. At pH 13, where all the surface functional groups are ionized to silanolate (SiO−), the magnitude of the $B\Psi([\sigma])$ will be proportional to the number of empty sites at the silica surface. Indeed, the sample shows a decreased surface electric potential at pH 13 and, therefore, a decreased number of surface empty sites, compared with that of bare silica. The results from *N*,*N*-(dimethylamino)trimethylsilane are shown in Figure 4. From Figure 4 it is clear that not all the surface functional groups are converted into inert $-Si(CH_3)_3$ moieties. Assuming a constant capacitor electric double-layer model,[13] one can roughly estimate, from the electric potential decrease after a SAM is formed, that only about 50% of the total surface silanol −SiOH groups reacted with an organosilane, under our experimental conditions. The quantitative estimation for the SAM coverage may vary if another electric double-layer model is imposed.

References and Notes

(1) Kumar, A.; Abbott, N. L.; Kim, E.; Biebuyck, H. A.; Whitesides, G. M. *Acc. Chem. Res.* **1995**, *28*, 219−226.
(2) Eisenthal, K. B. *Annu. Rev. Phys. Chem.* **1992**, *43*, 627−661.
(3) Eisenthal, K. B. *Acc. Chem. Res.* **1993**, *26*, 636−643.
(4) Mrksich, M.; Whitesides, G. M. *Trends Biotechnol.* **1995**, *13*, 228−235.
(5) Arkles, B. *Chemtech* **1977**, *7*, 766.
(6) *Silicon, Germanium, Tin and Lead Compounds Metal Alkoxides, Diketonates and Carboxylates-A Survey of Properties and Chemistry*; Arkles, B., Ed.; Gelest, Inc.: Tullytown, PA, 1995; p 49.
(7) Tillman, N.; Ulman, A.; Schildkraut, J. S.; Penner, T. L. *J. Am. Chem. Soc.* **1988**, *110*, 6136.
(8) Legrange, J. D.; Markham, J. L.; Kurkjian, C. R. *Langmuir* **1993**, *9*, 1749−1753.
(9) Zhao, X.; Kopelman, R. *J. Phys. Chem.* **1996**, *100*, 11014.
(10) Schmitz, I.; Schreiner, M.; Friedbacher, G.; Grasserbauer, M. *Anal. Chem.* **1997**, *69*, 1012.
(11) Ong, S. W.; Zhao, X. L.; Eisenthal, K. B. *Chem. Phys. Lett.* **1992**, *191*, 327−335.
(12) Zhao, X. L.; Ong, S. W.; Eisenthal, K. B. *Chem. Phys. Lett.* **1993**, *202*, 513−520.
(13) Adamson, A. W. *Physical Chemistry of Surfaces*; Wiley: New York, 1990.
(14) Frisch, H. L.; Mysels, K. J. *J. Phys. Chem.* **1983**, *87*, 3988−3990.
(15) Szabo, K.; Ha, N. L.; Schneider, P.; Zeltner, P.; Kovats, E. S. *Helv. Chim. Acta* **1984**, *67*, 2128.
(16) Evans, J. W. *Rev. Mod. Phys.* **1993**, *65*, 1281.
(17) Kang, H. L.; Weinberg, W. H. *Acc. Chem. Res.* **1992**, *25*, 253.
(18) Havlin, S.; Ben-Avraham, D. *Adv. Phys.* **1987**, *36*, 695.
(19) Family, F.; Meakin, P. *Phys. Rev. A* **1987**, *40*, 3836.
(20) Lindenberg, K.; Romero, A. H.; Sancho, J. M.; Sagues, F.; Reigada, R.; Lacasta, A. M. *J. Phys. Chem.* **1996**, *100*, 19066.